Synchronization between two weakly coupled delay-line oscillators

Etgar C. Levy* and Moshe Horowitz†
Department of Electrical Engineering, Technion–Israel Institute of Technology, Haifa 32000, Israel
(Received 12 August 2012; published 19 December 2012)

We study theoretically the generation of a continuous-wave signal by two weakly coupled delay-line oscillators. In such oscillators, the cavity length is longer than the wavelength of the signal. We show by using an analytical solution and comprehensive numerical simulations that in delay-line oscillators, the dynamics of the amplitude response cannot be neglected even when the coupling between the oscillators is weak. Therefore, weakly coupled delay-line oscillators cannot be accurately modeled by using coupled phase-oscillator models. In particular, we show that synchronization between the oscillators can be obtained in cases that are not allowed by coupled phase-oscillator models. We study the stability of the continuous-wave solutions. In delay-line oscillators, several cavity modes can potentially oscillate. To ensure stability, the bandwidth of the delay-line oscillator should be limited. We show that the weakly coupled delay-line oscillator model that is described in this paper can be used to accurately model the synchronization between two weakly coupled optoelectronic oscillators. A very good quantitative agreement is obtained between a comprehensive numerical model to study optoelectronic oscillators and the model results given in this paper.

DOI: 10.1103/PhysRevE.86.066209 PACS number(s): 05.45.Xt, 85.60.−q

I. INTRODUCTION

Synchronization between two coupled oscillators has been studied extensively in many fields [1–21]. Two self-sustained oscillators which oscillate autonomously with different natural frequencies can start oscillating with a common frequency even if they interact weakly with each other [1–5]. Many studies on synchronization were performed by using coupled phase-oscillator models that consider only the dynamics of the oscillator phases, and ignore the amplitude dynamics. Such models were justified when the coupling is weak and hence the amplitude change is small and can therefore be neglected [6]. One of the most well-known models for coupled phase oscillators is the Kuramoto model [7]. Collective behavior of coupled phase-oscillator systems was studied extensively [7,8]. The original Kuramoto model is based on the assumption that the coupling between the oscillators is instantaneous. The effect of a finite time delay on the coupling between phase oscillators has been widely studied by extending the Kuramoto model [8–13]. When the coupling is strong, the amplitude response of the oscillators must be retained to describe new phenomena such as amplitude death [6,14,15].

In this paper, we analyze the synchronization between two weakly coupled delay-line oscillators. Delay-line oscillators are embedded with a feedback path that has a loop delay τ. We show that the amplitude response is required to model such weakly coupled delay-line oscillators. Thus, weakly coupled delay-line oscillators cannot be accurately modeled by coupled-phase-oscillator models. Our study shows that when the coupling adds a $\pi/2$ phase, there are two terms that contribute to the synchronization region, a term that is linearly dependent on the coupling parameter, and another term that is quadratically dependent on the coupling parameter. While the linear term contribution to the synchronization region is well known from phase-oscillators models, the quadratic term contribution was not analyzed. The physical effect of the quadratic term enables two delay-line oscillators to get synchronized under conditions that only the linear term would not allow. We show the conditions under which the quadratic term dominates the synchronization region for two similar delay-line oscillators. We study the small-signal stability of the solutions. The presence of low-intensity cavity modes should be taken into account in the stability analysis of the solution.

The effect of synchronization between oscillators has an important consequences for practical implementations, such as coupled electrical oscillators [1–5] and coupled lasers [16–21]. In this paper, we apply the theory to another important application—two weakly coupled optoelectronic oscillators (OEOs). OEOs are hybrid devices that contain both electrical and optical components [22]. The amplification is obtained by using an rf amplifier and a long optical fiber is used as a high-Q cavity. An electro-optic modulator is used to convert the rf signal into light modulation. The nonlinear transfer curve of the modulator often determines the gain saturation. OEOs can oscillate in several cavity modes. Locking of two OEOs is used to prevent mode-hopping and to improve the OEO performance [23,24]. In a previous work, we have developed a comprehensive numerical simulation to study the coupling between two OEOs [25]. A very good quantitative agreement was obtained between the comprehensive numerical simulation and the experimental results [25]. We show that the results of the comprehensive numerical simulation for two weakly coupled OEOs are in good quantitative agreement with the results of the weakly coupled delay-line oscillator model that is presented in this paper. We used the delay-line oscillator model to study the conditions under which a synchronized continuous-wave signal can be obtained by two weakly coupled OEOs. We analyze the effect of the coupling phase on the synchronization properties of OEOs. In particular, we explain why two identical OEOs that are weakly coupled to each other can be synchronized. This result is not obtained by using phase-oscillator models.

*etgarlevy@gmail.com
†horowitz@ee.technion.ac.il

Chaos synchronization in coupled OEOs has been studied in previous works, such as [26–28]. The coupled OEOs were used to study potential applications such as chaos-based communications and secure communications with chaos. However, these works do not refer to the continuous-wave solution and do not study the conditions under which such a solution can be obtained by weakly coupled OEOs. Chaotic behavior of a single-loop OEO can be obtained by increasing its small-signal open-loop gain [29,30], and can be avoided by limiting the intracavity filter bandwidth [30]. In this paper, the small-signal open-loop gain of each of the OEOs is assumed to be small enough such that a continuous-wave signal is obtained when the OEOs are not coupled.

The rest of this paper is organized as follows: In Sec. II, we describe the model of weakly coupled delay-line oscillators and show the derivation of the weakly coupled differential equations. In Sec. III, we derive an analytical solution for the cases of the zero- and the $\pi/2$-coupling phase. In Sec. IV, we demonstrate the results in two similar delay-line oscillators that are coupled to each other in the case of the zero- and the $\pi/2$-coupling phase. In Sec. V, we describe a comparison of the analytical results to the comprehensive numerical simulation results that was developed to study coupled OEOs, and in Sec. VI we describe the small-signal stability analysis of the obtained solutions. We finally conclude in Sec. VII.

II. THEORETICAL FRAMEWORK

A schematic description of the system that we model is shown in Fig. 1. The system consists of two coupled delay-line oscillators. Each of the two oscillators ($j = 1,2$) contains a saturable amplifier, a loop delay τ_j, and a filter with a frequency response, $F_j(\omega) = |F(\omega)| \exp[i\varphi_j^F(\omega)]$. In the absence of coupling, each of the oscillators is a self-sustained oscillator that generates a continuous-wave signal with a frequency ω_j, which is referred to as the natural frequency of the jth oscillator. In general, the Barkhausen condition for the natural frequencies implies that $\omega_j\tau_j - \varphi_j^F(\omega_j) = 2\pi N_j$, where N_j is an integer and τ_j are the loop delay in the oscillators. For the sake of simplicity, the loop delay of the oscillators τ_j is defined without the loss of generality, such that $\varphi_j^F(\omega_j) = 0$. Therefore, the Barkhausen condition for the natural frequencies is $\omega_j\tau_j = 2\pi N_j$ [31]. The oscillating signal in each of the two uncoupled oscillators can be described by

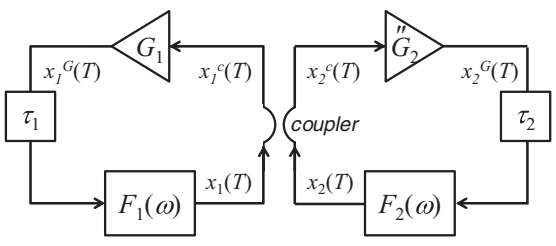

FIG. 1. Schematic description of the weakly coupled delay-line oscillators model. Each of the delay-line oscillators contains a saturable amplifier with a saturable gain $x_j^G(T) = G_j[|x_j^c(T)|]x_j^c(T)$, a delay line τ_j, and a filter with a frequency response, $F_j(\omega)$. $x_j(T)$, $x_j^c(T)$, and $x_j^G(T)$ are the signals before the coupler, after the coupler, and after the saturable amplifier, respectively. The dynamic equations for the oscillating signal are given by Eqs. (5).

by

$$\begin{aligned} s_j(t,T) &= |x_j(T)|\cos[\omega_j t + \phi_j(T)] \\ &= x_j(T)\exp(i\omega_j t)/2 + \text{c.c.}, \end{aligned} \tag{1}$$

where t is a fast time scale on the order of $t \sim \omega_j^{-1}$, T is a slow time scale on the order of the loop delay $T \sim \tau_j$, $\phi_j(T)$ is the phase of the oscillating signal, and $x_j(T) = |x_j(T)|\exp[i\phi_j(T)]$ is the phasor of the oscillating signal $s_j(t,T)$. We assume that the complex signal envelope, $x_j(T)$, is slowly varying in compare with the natural frequency: $d\phi_j/dT \ll \omega_j$ and $d|x_j|/dT \ll |x_j|\omega_j$.

The coupling between the two delay-line oscillators is described by

$$\begin{pmatrix} x_1^c(T) \\ x_2^c(T) \end{pmatrix} = \begin{pmatrix} s_{11} & s_{12} \\ s_{21} & s_{22} \end{pmatrix} \begin{pmatrix} x_1(T) \\ x_2(T) \end{pmatrix}, \tag{2}$$

where $x_j(T)$ and $x_j^c(T)$ are defined as the complex envelopes of the oscillating signals before and after the coupling, respectively, and $s_{j,j} = \rho_j\exp(i\theta_j)$, $s_{j,3-j} = \kappa_j\exp(i\psi_j)$, are the complex coupling coefficients. The coupling between the two oscillators is linear and is frequency-independent.

We are interested in the conditions under which frequency entrainment is obtained, such that the two oscillators oscillate with a common frequency, ω_0. Our theoretical framework is based on the following assumptions: (a) The saturable amplifier has an instantaneous response and the nonlinear transfer function of the amplifier can be described by $G_j[|x_j^c(T)|]$, where $x_j^c(T)$ is the complex envelope of the signal at the input port of the amplifier. (b) The bandwidth of each of the filters is much narrower than the corresponding natural frequencies. As a result, the complex signal envelope, $x_j(T)$, is slowly varying in comparison with the carrier period: $d\phi_j/dT \ll \omega_j$ and $d|x_j|/dT \ll |x_j|\omega_j$. (c) The relative change in the phasor of the oscillating signal from one round trip to the following is small in each of the two oscillators. This assumption implies a weak coupling, such that $\kappa_j|x_j|/(\rho_n|x_n|) \ll 1$, $n = 1,2$ $j = 3-n$. (d) The model neglects processes that convert phase modulation to amplitude modulation and vice versa.

According to assumption (c), the oscillating signal can be regarded as a quasiperiodic signal [32], and as a result can be expanded as

$$x_j^c(T) = \sum_{m=-\infty}^{\infty} a_{m,j}(T)\exp\{i[\Omega_{m,j}T + \phi_{m,j}(T)]\}, \tag{3}$$

where $a_{m,j}\exp(i\phi_{m,j})$ denote the Fourier coefficients, m is an integer number, and $\Omega_{m,j} = 2\pi m/\tau_j$.

In this paper, we are interested in a continuous-wave (CW) solution for the oscillating signals, s_j, in which most of the signal energy is contained in a single oscillating mode, and hence $a_{0,j}^2(T) \gg \sum_{m\neq 0} a_{m,j}^2(T)$. We denote $m = 0$ as the index of the oscillating mode, and $m \neq 0$ as the indices of the low-intensity modes. Therefore, the amplitudes and the phases of the oscillating signals can be approximated by

$$\begin{aligned} u_j(T) &\equiv |x_j^c(T)| \approx a_{0,j}(T), \\ \phi_j(T) &\approx \phi_{0,j}(T), \end{aligned} \tag{4}$$

respectively. According to Appendix A, the dynamic equations for the oscillating mode are

$$\begin{aligned}\dot{u}_n &= u_n[\rho_n V_n(u_n)/u_n - 1]/\tau_n + [\kappa_j V_j(u_j)/\tau_n]\cos(\gamma_{jn}),\\ \dot{\phi}_n &= \omega_n - \omega_0 - (k_{jn}/\tau_n)\sin(\gamma_{jn}) + \theta_n/\tau_n,\end{aligned} \tag{5}$$

where $n = 1,2$ is the oscillator index, $j = 3 - n$, $\dot{u}_n$ is the time derivative of u_n with respect to the long time scale, T, τ_j are the loop delays, $V_j(u_j) = G_j(u_j)u_j$ are the amplitudes at the amplifiers output, $G_j(u_j)$ are the nonlinear amplifier response, $k_{jn}(T) = \kappa_j V_j[u_j(T)]/[\rho_n V_n[u_n(T)]]$,

$$\gamma_{jn} = \omega_0(\tau_j - \tau_n) - \psi_j + \theta_n + (-1)^n \Delta\phi, \tag{6}$$

$\Delta\phi = \phi_2 - \phi_1$, and the weak-coupling approximation requires $k_{jn} \ll 1$. In deriving Eqs. (5), it is assumed that $F(\omega) \approx 1$ for the oscillating mode $\omega \approx \omega_0$.

A. Analogy to the coupled phase-oscillator model

In previous works, it was assumed that when the coupling between two oscillators is weak, the coupled oscillators can be modeled as phase oscillators, in which only the oscillator phase is used to describe the dynamics of the oscillators [6]. In this case, the amplitudes of two weakly coupled self-sustained oscillators are assumed to be equal to the free-running amplitudes, such that $u_j = u_j^0$, when u_j^0 are the free-running amplitudes, $j = 1,2$.

The two coupled equations for the phase dynamic in the delay-line oscillators that were given in Eqs. (5) look similar to the well-known coupled phase-oscillator equations [7–13] if we set $\theta_j = 0$, $u_j = u_j^0$ and use

$$\varphi_j = \omega_0 t + \phi_j, \tag{7}$$

such that

$$\begin{aligned}\dot{\varphi}_1 &= \omega_1 - k_{21}^0/\tau_1 \sin[\varphi_1(t_1) - \varphi_2(t_2) - \psi_2],\\ \dot{\varphi}_2 &= \omega_2 - k_{12}^0/\tau_2 \sin[\varphi_2(t_2) - \varphi_1(t_1) - \psi_1],\end{aligned} \tag{8}$$

where $k_{jn}^0 = \kappa_j u_j^0/u_n^0$, $t_j = t - \tau_j$. A major difference between Eqs. (5) and (8) is that the coupling parameters in Eqs. (5), k_{jn}, are in general a function of the oscillating amplitudes, u_j. This is in contrast to the Kuramoto model and other phase-oscillator models [4], in which it is assumed that the oscillating amplitudes in the synchronized state are equal to the free-running amplitudes, $u_j = u_j^0$, and the coupling parameters are therefore constants. We shall show that the amplitude dynamics, which is present in Eqs. (5) and is missing from the coupled phase-oscillator model, is required to accurately describe the synchronization region of two similar weakly coupled delay-line oscillators that are coupled with a coupling phase of $\psi_j = \pi/2$, $j = 1,2$.

B. Phasor dynamic equations with long time-scale parameters

The synchronous CW solutions of the weakly coupled delay-line oscillators can be found by setting $\dot{u}_j = \dot{\phi}_j = 0$ in Eqs. (5). In this case, Eqs. (5) have four unknowns: u_j, the amplitudes of the oscillating signals; $\Delta\phi$, the relative phase between the signals; and ω_0, the common angular frequency when the two oscillators are synchronized to each other. The parameters of Eqs. (5) are the loop delays, τ_j, the coupling coefficients, s_{nj}, and the nonlinear response of the saturable amplifier, $G_j(u_j)$.

The loop delays, τ_j, and the common oscillation frequency, ω_0, can belong to different time scales in delay-line oscillators. For example, for a typical OEO, the oscillation frequency is about 10 GHz while the loop delays are of the order of 0.1–10 μs. The different time scales in Eqs. (5) make it inconvenient to be solved. Thus, to calculate the parameter $\omega_0\tau_j$ in Eqs. (5) with an accuracy of 1%, the loop delay should be specified with an accuracy of 10^{-5}–10^{-7}. To overcome this inconvenience, we shall transform Eqs. (5) into equations without the short time scale of the common frequency. We define the frequency shift of the common frequency in synchronization from the mean of the natural frequencies, $\Omega = \omega_0 - (\omega_1 + \omega_2)/2$. Since according to the Barkhausen condition the natural frequencies satisfy $\omega_j\tau_j = 2\pi N_j$ such that N_j is an integer [31], we get that

$$\begin{aligned}\dot{u}_1 &= u_1[\rho_1 V_1(u_1)/u_1 - 1]/\tau_1 + [\kappa_2 V_2(u_2)/\tau_1]\cos(\tilde{\gamma}_{21}),\\ \dot{u}_2 &= u_2[\rho_2 V_2(u_2)/u_2 - 1]/\tau_2 + [\kappa_1 V_1(u_1)/\tau_2]\cos(\tilde{\gamma}_{12}),\\ \dot{\phi}_1 &= -(\Omega + \Delta\omega) - (k_{21}/\tau_1)\sin(\tilde{\gamma}_{21}) + \theta_1/\tau_1,\\ \dot{\phi}_2 &= -(\Omega - \Delta\omega) - (k_{12}/\tau_2)\sin(\tilde{\gamma}_{12}) + \theta_2/\tau_2,\end{aligned} \tag{9}$$

where

$$\begin{aligned}\tilde{\gamma}_{12} &= (\Omega + \Delta\omega)\tau_1 - (\Omega - \Delta\omega)\tau_2 - \psi_1 + \theta_2 + \Delta\phi,\\ \tilde{\gamma}_{21} &= (\Omega - \Delta\omega)\tau_2 - (\Omega + \Delta\omega)\tau_1 - \psi_2 + \theta_1 - \Delta\phi,\end{aligned} \tag{10}$$

and the detuning frequency is defined as the frequency difference between the two natural frequencies, $2\Delta\omega = \omega_2 - \omega_1$.

III. ANALYTIC SOLUTION FOR A SINGLE-MODE OSCILLATION

In this section, we derive analytic solutions for two similar weakly coupled delay-line oscillators. We consider the case in which the two delay-line oscillators have the same saturation curve, $G_j(u_j) = G(u_j)$, $j = 1,2$, and the coupling parameters satisfy $\kappa_j = \kappa \ll 1$, $\rho_j \cong 1$, $\theta_j = 0$, and $\psi_j = \psi$ for $j = 1,2$. The analytic solutions are derived for the zero-coupling phase, $\psi = 0$, and for the $\pi/2$-coupling phase, $\psi = \pi/2$. The filter bandwidth is assumed to be narrow enough such that the solution is stable, as discussed in Sec. VI B.

In deriving the solutions we do not omit the amplitude dynamics, as is done in phase-oscillator models. We denote the free-running amplitude of the two uncoupled oscillators by u_j^0. Since we consider the case of two similar delay-line oscillators with the same nonlinear response of the saturable amplifier $V_j(u) = V(u)$, the free-running amplitudes are equal to each other, $u_j^0 = u^0$. We assume that due to the weak coupling the deviation of the oscillating amplitude is small such that the amplitudes of the coupled oscillators equal

$$u_j = u^0 + \Delta u_j, \tag{11}$$

and $\Delta u_j/u^0 \ll 1$. This assumption is verified in Sec. IV by solving numerically Eqs. (9). The amplitudes at the output of the amplifiers are given by

$$V(u_j) = u^0 + V'(u^0)\Delta u_j, \tag{12}$$

where $V'(u) = dV(u)/du$. We note that $V'(u^0) < 1$ since u^0 is an amplitude of the free-running oscillators that are assumed to be stable to amplitude noise [31]. We denote the ratio between the amplified amplitudes by

$$V(u_1)/V(u_2) = 1 + \delta_u. \tag{13}$$

We calculate δ_u in the following subsections. We show that for the zero-coupling phase, $\delta_u = 0$, and the amplitude dynamics has no effect on the synchronization region, and therefore it can be omitted. The synchronization region in this case has a linear dependence on the coupling parameter. However, for the $\pi/2$-coupling phase, $\delta_u \neq 0$ and the amplitude dynamics contributes to the synchronization region a term that depends on the square of the coupling parameter.

A. Zero-coupling phase

We substitute Eq. (12) in the two first equations of Eqs. (9), and we set $\dot{u}_j = 0$ and $\psi = 0$ and obtain

$$\begin{aligned}(V'-1)\Delta u_1 + \kappa V'\cos(\Delta\zeta)\Delta u_2 &= -\kappa u^0\cos(\Delta\zeta),\\ \kappa V'\cos(\Delta\zeta)\Delta u_1 + (V'-1)\Delta u_2 &= -\kappa u^0\cos(\Delta\zeta),\end{aligned} \tag{14}$$

where $V' = V'(u^0)$ and

$$\Delta\zeta = \Delta\phi - \Omega(\tau_1 - \tau_2) + \Delta\omega(\tau_1 + \tau_2) \tag{15}$$

is the generalized phase difference. Solving Eqs. (14) for the amplitude deviations, we get that $\Delta u_1 = \Delta u_2$. As a result, $V(u_1)/V(u_2) = 1$, and therefore $\delta_u = 0$.

We continue by calculating the common frequency, Ω, the generalized phase, $\Delta\zeta$, and the synchronization region, $2\Delta\omega_{\max}$. We set $\dot{\phi}_j = 0$, $\psi = 0$ and obtain

$$2\Delta\omega\tau = 2\kappa\sin(\Delta\zeta) \tag{16}$$

and

$$\Omega\tau = -\kappa\delta_\tau\sin(\Delta\zeta), \tag{17}$$

where τ is the harmonic average of the loop delays,

$$\tau^{-1} = \left(\tau_1^{-1} + \tau_2^{-1}\right)/2, \tag{18}$$

and $2\delta_\tau$ is the normalized loop-delay difference,

$$\delta_\tau = (\tau_1 - \tau_2)/(\tau_1 + \tau_2). \tag{19}$$

The synchronization region is derived from Eq. (16) by requiring that $|\sin(\Delta\zeta)| \leqslant 1$:

$$2\Delta\omega_{\max}\tau = 2\kappa. \tag{20}$$

In this case, the synchronization region has a linear dependence on the coupling parameter. The analytic solution for the common frequency, Ω, and the phase difference, $\Delta\phi$, is given by

$$\Omega = -\delta_\tau\Delta\omega \tag{21}$$

and

$$\Delta\phi = \arcsin\left(\Delta\omega\tau/\kappa\right) + \Omega(\tau_1 - \tau_2) - \Delta\omega(\tau_1 + \tau_2). \tag{22}$$

B. $\pi/2$-coupling phase

We now consider the case in which the coupling phase equals $\psi = \pi/2$. This case is important to describe a coupling that is energy-preserving. The sufficient and necessary conditions that the coupling parameters should satisfy for an energy-preserving coupler are as follows [33,34]: $|s_{11}| = |s_{22}|$, $|s_{21}| = |s_{12}|$, $|s_{11}|^2 + |s_{21}|^2 = 1$, and $s_{11}s_{21}^* + s_{22}^*s_{12} = 0$. Thus, we set $s_{21} = s_{12} = i\kappa$ and $s_{11} = s_{22} = \sqrt{1-\kappa^2}$, and therefore $\theta_j = 0$ and $\psi_j = \psi = \pi/2$.

By using a similar derivation as used for the zero-coupling phase, we obtain that for $\psi = \pi/2$,

$$\Delta u_n = (-1)^{n-1}\kappa u^0\sin(\Delta\zeta)/(V'-1) \tag{23}$$

and

$$\delta_u = \frac{-\delta_G\kappa\sin(\Delta\zeta)}{1 + \delta_G\kappa\sin(\Delta\zeta)/2}, \tag{24}$$

where $\delta_G = (2V')/(1-V') = 2(1+G'u^0)/(-G'u^0)$.

We set $\dot{\phi}_j = 0$ and $\psi = \pi/2$ in Eqs. (9) and obtain

$$2\Delta\omega\tau = -2\kappa\cos(\Delta\zeta)\left[\delta_\tau - \frac{\delta_G\kappa\sin(\Delta\zeta)}{1 + \delta_G\kappa\sin(\Delta\zeta)/2}\right] \tag{25}$$

and

$$\Omega\tau = \kappa\cos(\Delta\zeta)\left[1 - \frac{\delta_\tau\delta_G\sin(\Delta\zeta)}{1 + \delta_G\kappa\sin(\Delta\zeta)/2}\right], \tag{26}$$

where τ and δ_τ are given by Eqs. (18) and (19), respectively. We see that in this case there are two terms that contribute to the synchronization region. The first term in Eq. (25) has a linear dependence on the coupling parameter, and the second term has a quadratic dependence on the coupling parameter. The contribution of the quadratic term does not exist in phase-oscillator models that omit the amplitude dynamics and assume $u_j = u_j^0$.

When the normalized difference in the loop delays is sufficiently greater than zero, such that $|\delta_\tau|/(\delta_G\kappa) \gg 1$, the quadratic term in Eq. (25) can be neglected and

$$2\Delta\omega\tau \approx -2\delta_\tau\kappa\cos(\Delta\zeta). \tag{27}$$

The synchronization region in this case is given by

$$2\Delta\omega_{\max}\tau = 2\delta_\tau\kappa. \tag{28}$$

Thus, the synchronization region has a linear dependence on the coupling term when the two loop delays, τ_1 and τ_2, are sufficiently different from each other, such that $|\delta_\tau|/(\delta_G\kappa) \gg 1$.

However, when the two loop delays are sufficiently similar to each other, such that $|\delta_\tau|/(\delta_G\kappa) \ll 1$, the linear term in Eq. (25) can be neglected and

$$2\Delta\omega\tau \approx \delta_G\kappa^2\sin(2\Delta\zeta). \tag{29}$$

The synchronization region in this case is given by

$$2\Delta\omega_{\max}\tau = \delta_G\kappa^2. \tag{30}$$

An analytic solution for the common frequency, Ω, and the phase difference, $\Delta\phi$, can be derived in cases in which $|\delta_\tau|/(\delta_G\kappa) \ll 1$ and $\delta_\tau\delta_G \ll 1$, by using Eqs. (25) and (26):

$$\Omega \approx \pm\frac{\kappa}{\tau}\sqrt{\frac{1 \pm \sqrt{1 - [(2\Delta\omega\tau)/(\delta_G\kappa^2)]^2}}{2}} \tag{31}$$

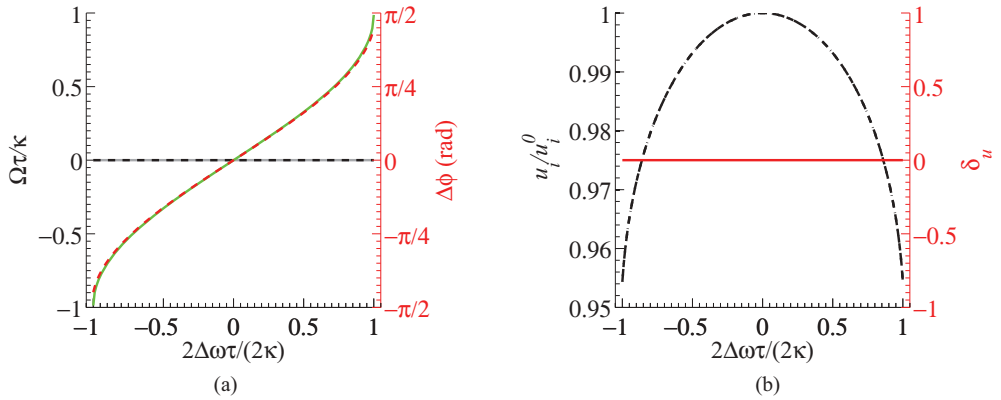

FIG. 2. (Color online) (a) Normalized common frequency $\Omega\tau/\kappa$ (black-dashed line) and the phase difference between the oscillators $\Delta\phi$ (red-dashed line) and (b) normalized amplitudes, u_1/u_1^0 (black dashed-dotted line), u_2/u_2^0 (black-dashed line), and the parameter δ_u (red solid line), as a function of the normalized frequency detuning, $2\Delta\omega\tau/(2\kappa)$, for the case of the zero-coupling phase, $\psi_j = 0$, calculated by solving the differential equations, Eqs. (9). The analytical solutions for the normalized common frequency (gray-solid line) and the phase difference (green-solid line) are calculated by using Eqs. (21) and (22), respectively, and are shown in Fig. 2(a). The parameters that are used in this example are $u_j^0 \simeq 0.866$, $\tau_j = 0.25\ \mu$s, $G_{S,j} = 1.1$, $\theta_j = 0$, $\kappa_j = \kappa = 0.01$, and $\rho_j = 1 - \kappa$ for $j = 1,2$.

and

$$\Delta\phi \approx \arcsin\left[(2\Delta\omega\tau)/(\delta_G\kappa^2)\right]/2 + \Omega(\tau_1 - \tau_2) - \Delta\omega(\tau_1 + \tau_2). \quad (32)$$

We shall see in Sec. VI that the solution branch in Eq. (31) which satisfies $\Omega = 0$ when $\Delta\omega = 0$ is not stable.

IV. EXAMPLES FOR WEAK COUPLING BETWEEN TWO SIMILAR DELAY-LINE OSCILLATORS

In this section, we solve two examples that demonstrate the model results that were described in Sec. III. We numerically solve Eqs. (9) and compare the solution to the analytic solutions that are described in Sec. III. We perform this comparison for both the zero- and the $\pi/2$-coupling phase.

To solve Eqs. (9), it is required to define the gain saturation function. The examples given in this section are calculated for a nonlinear response function of the saturable amplifier that is given by

$$G_j(u_j) = 2G_{S,j}J_1(u_j)/u_j, \quad (33)$$

where $G_{S,j}$ is a parameter that represents the small-signal open-loop gain, and J_1 is the first-order Bessel function. As is described in Sec. V, such a nonlinear response corresponds to the response of a Mach-Zehnder modulator that can be used to model coupled OEOs.

We studied the case of the zero- and the $\pi/2$-coupling phase, $\psi = 0$ and $\psi = \pi/2$, respectively. As ψ was increased from 0 to $\pi/2$, the synchronization region decreased monotonically and the effect of the amplitude dynamic on the synchronization region was increased.

A. Zero-coupling phase

Figure 2 shows the synchronous CW solution, calculated by solving numerically Eqs. (9) for the zero-coupling phase, $\psi_j = \psi = 0$. The analytic solutions calculated by using Eqs. (21) and (22) are also given for comparison. The parameters of the delay-line oscillators and the coupling coefficients are $\tau_j = 0.25\ \mu$s, $G_{S,j} = 1.1$, $\theta_j = 0$, $\kappa = 0.01$, and $\rho_j = 1 - \kappa$ for $j = 1,2$. A good quantitative agreement is achieved between the analytic and the numerical solutions of Eqs. (9). The analytic results indicate that the synchronization region equals $|2\Delta\omega_{\max}| = 2\kappa/\tau$, and that the common frequency is equal to the mean of the natural frequencies, $\Omega = 0$, in accordance with Eqs. (20) and (17), respectively. The oscillation amplitudes in the analytic solutions are equal to each other, $u_1 = u_2$, all over the synchronization region. The numerical solution of Eqs. (9) shows that for zero detuning, $2\Delta\omega = 0$, the oscillation amplitudes are equal to the natural amplitudes of the oscillators in the absence of the coupling, $u_j = u_j^0$, where $u_j^0 \simeq 0.866$. The amplitudes decrease as the absolute frequency detuning increases. The decrease in the amplitudes suggests that the total energy in the coupled system, which is proportional to $E = |u_1^2| + |u_2^2|$, decreases as the absolute frequency detuning increases.

B. $\pi/2$-coupling phase

Figure 3 shows the synchronous CW solution to Eqs. (9) when the coupling phase equals $\pi/2$, $\psi_j = \psi = \pi/2$. The analytic solutions calculated by using Eqs. (31) and (32) are also given for comparison. The rest of the parameters, unless otherwise specified, are identical to that used in the case of the zero-coupling phase that is shown in Fig. 2 and hence $\delta_\tau = 0$ and $\delta_G \approx 8$. Figure 3 indicates that the synchronization region that is obtained is in accordance with the analytic solution given in Eq. (30). Unlike in the zero-coupling-phase case, the common frequency varies within the synchronization region. For a zero detuning, $\omega_1 = \omega_2$, the common frequency is given by $\Omega = \pm\kappa/\tau$—thus, it is located outside the frequency region $[\omega_1,\omega_2]$. This result is also in accordance with the analytic result that is given in Eq. (31), as $\delta_\tau = 0$. In Sec. IV, we shall show that this solution is stable. There exists another solution of Eq. (9) with a common frequency that is given by $\Omega = 0$. In Sec. IV, we shall show that this solution is unstable to phase perturbations when $\tau_1 = \tau_2$, $\psi = \pi/2$, and $\Delta\omega = 0$. A stable solution for synchronization between two identical

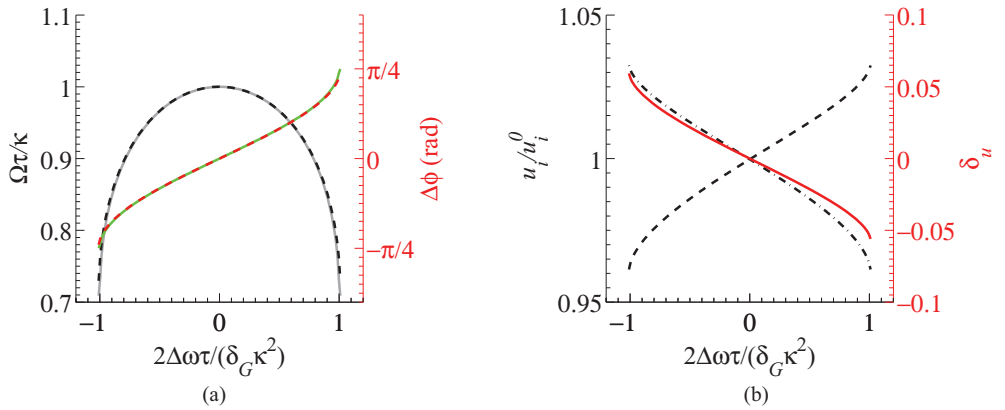

FIG. 3. (Color online) (a) Normalized common frequency $\Omega\tau/\kappa$ (black-dashed line) and the phase difference between the oscillators $\Delta\phi$ (red-dashed line) and (b) normalized amplitudes, u_1/u_1^0 (black dashed-dotted line), u_2/u_2^0 (black-dashed line), and the parameter δ_u (red solid line), as a function of the normalized frequency detuning, $2\Delta\omega\tau/(\delta_G\kappa^2)$, for the case of the $\pi/2$-coupling phase, $\psi_j = \pi/2$, calculated by solving the differential equations, Eqs. (9). The analytical solutions of the normalized common frequency (gray-solid line) and the phase difference (green-solid line) are calculated by using Eqs. (31) and (32), respectively, and are shown in Fig. 3(a). The parameters that are used in this example are $u_j^0 \simeq 0.866$, $\tau_j = 0.25\ \mu$s, $G_{S,j} = 1.1$, $\theta_j = 0$, $\kappa_j = \kappa = 0.01$, and $\rho_j = (1-\kappa^2)^{1/2}$ for $j = 1,2$.

oscillators, $\omega_1 = \omega_2$, that are coupled with a $\pi/2$-coupling phase to each other is not possible according to the phase-oscillator models, which assume symmetrical instantaneous coupling [4]. However, the example given in this paper shows that such oscillators can be locked with a common frequency located outside the frequency region $[\omega_1,\omega_2]$.

Figure 3(b) shows that the oscillation amplitudes, u_j, vary monotonically with the frequency detuning. As a result, $\delta_u \neq 0$ when $\Delta\omega \neq 0$. The amplitudes vary such that the total energy that is stored in the oscillators, E, remains constant due to the $\pi/2$-coupling phase.

V. COMPARISON TO A COMPREHENSIVE NUMERICAL SIMULATION OF COUPLED OPTOELECTRONIC OSCILLATORS

In this section, we show that the model for weakly coupled delay-line oscillators that is described in this paper accurately describes the synchronization between two weakly coupled OEOs. We compare the analytic solutions for the synchronization region, which are given in Eq. (20) and Eq. (25), to the results of a comprehensive numerical simulation for coupled OEOs. The comprehensive numerical simulation and a schematic description of the coupled OEOs are described in detail in [25] (Fig. 3): each OEO contains an optical fiber, an rf filter, a laser, an electro-optic modulator, a photodetector, and an rf amplifier. Light from a laser is fed into an electro-optic modulator, which converts microwave signals into a modulation of the light intensity. The modulated light is sent through a long optical fiber and is then detected by using a photodetector, which converts the modulated light signal into an electrical signal. The electrical signal is then amplified, filtered, and is fed back into the electrical port of the modulator. In OEOs, the nonlinearity of the modulator and the nonlinearity of the amplifier are both instantaneous, and therefore it can be combined into a single nonlinear element. A long fiber is used as a delay line, which serves as the resonator, and determines the possible cavity modes. The rf filter is used to determine which modes can oscillate. The angular carrier frequencies, ω_j, are usually of the order of $2\pi \times 10$ GHz and the loop delay is usually of the order of 0.1–10 μs.

The OEO can be modeled according to the schematic description in Fig. 1 by presenting the electro-optic modulator, the photodetector, and the rf amplifier as a single saturable amplifier with a nonlinear response $G(u)$. We consider the case in which the electro-optic modulator is a Mach-Zehnder modulator (MZM) and the rf amplifier has a constant gain such that the nonlinear response of the amplifier and the MZM, $G(u)$, can be described by $G(u) = 2G_S J_1(\pi u/v_\pi)/(\pi u/v_\pi)$ [22], where G_S is the small-signal open-loop gain and v_π is the half-wave voltage of the MZM. The small-signal open-loop gain is determined by the parameters of the laser, the MZM, the photodetector, and the rf amplifier, as given in Appendix B. The length of the optical fiber determines the loop delay, τ_j, and the transmission spectrum of the rf filter determines $F_j(\omega)$. The coupling between the two OEOs is implemented by rf couplers, and it can therefore be modeled by Eq. (2).

The comprehensive numerical simulation of OEOs takes into account the location and the response of each of the lumped elements in each loop, and in particular the filter response and the nonlinear gain [25]. Noise is added to the oscillating signal in each round trip. The comprehensive numerical simulation does not require using assumptions such that the change in the signal in each round trip at any point in the loop is small or that the signal is narrowbanded relative to the filter bandwidth or that the coupling is weak. The comprehensive numerical simulation has been experimentally verified [25]. In this section, we shall show that a good agreement is achieved between the results of the comprehensive numerical simulation and the analytic solution for the synchronization region. The parameters of the comprehensive numerical simulation are given in Appendix B. The parameters were set such that $v_\pi = \pi$ and $G_S = 1.1$.

Figure 4(a) shows the synchronization region as a function of the squared coupling parameter, κ^2, according to the analytic solution in Eq. (30) when the normalized loop-delay difference

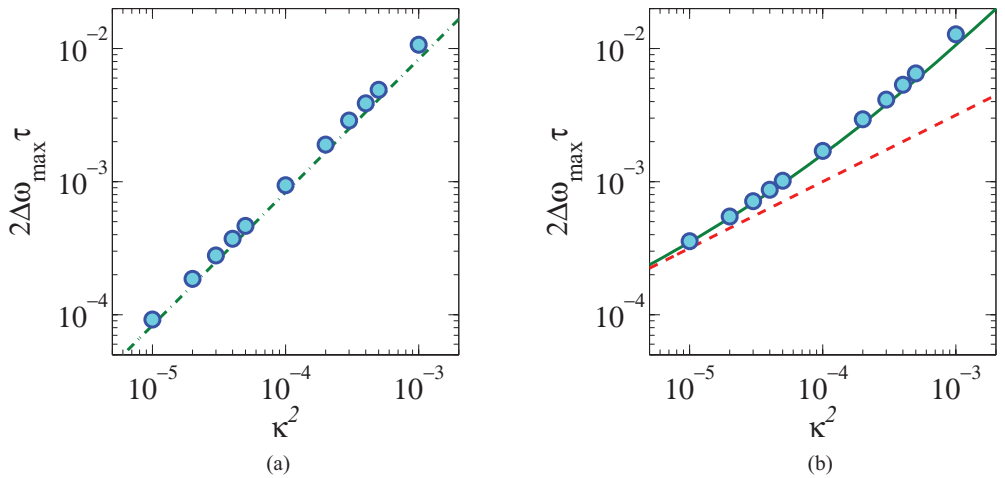

FIG. 4. (Color online) Synchronization region, $2\Delta\omega_{\max}\tau$, for a $\pi/2$-coupling phase, $\psi = \pi/2$, as a function of the squared coupling parameter, κ^2, for (a) $2\delta_\tau = 0$ and (b) $2\delta_\tau = 0.1$. The rest of the parameters are the same as in Fig. 3. The analytic results calculated by using Eq. (30) in (a) (green dashed-dotted line) and Eq. (25) in (b) (green solid line) are compared with the result of a comprehensive numerical simulation (cyan circles). The synchronization region in the phase-oscillator approximation equals zero in (a) and is shown in (b) by using Eq. (28) for $2\delta_\tau = 0.1$ (red dashed line).

equals zero, $2\delta_\tau = 0$. The results of the comprehensive numerical simulation are also presented for comparison. A good agreement is achieved between the analytical and the comprehensive numerical simulation results. It is shown that for two identical oscillators, the synchronization region is determined by the square of the coupling coefficient as obtained in Eq. (30).

Figure 4(b) shows the synchronization region as a function of the squared coupling parameter, κ^2, according to the solution of Eq. (25) when the normalized loop-delay difference equals $2\delta_\tau = 0.1$. A good agreement is achieved between the analytical and the comprehensive numerical simulation results. Figure 4(b) shows that for two similar oscillators, in which $0 < \delta_\tau \ll 1$, the synchronization region is approximately proportional to the coupling parameter when $\delta_G\kappa/|\delta_\tau| \ll 1$, and it is approximately proportional to the square of the coupling parameter when $\delta_G\kappa/|\delta_\tau| \gg 1$.

Figure 5 shows the synchronization region as a function of the normalized loop-delay difference, $2\delta_\tau$, according to Eqs. (25). The maximum discrepancy between the results of the comprehensive numerical simulation and the analytic solution is only about 5% for $\kappa = 0.01$ and $\delta_\tau = 0$. The figure shows that the synchronization region increases as the normalized loop-delay difference increases.

VI. SMALL-SIGNAL STABILITY ANALYSIS

In this section, we perform a small-signal stability analysis to the oscillating signal [35]. The small-signal stability of the solutions to the nonlinear equations can be determined by linearizing the equations around its solution. The presence of a loop delay in the oscillator plays a major role in determine whether the solution is stable or not. We divide the stability analysis in weakly coupled delay-line oscillators into two types: (a) instability due to amplitude and phase perturbations in the the oscillating mode; (b) instability due to excess gain in low-intensity cavity modes. By using the stability analysis, we have verified that all the examples that are given in Sec. IV are stable.

A. Small-signal stability analysis of the oscillating mode

Consider an oscillating signal in an uncoupled self-sustained oscillator, the amplitude and phase of which are subjected to perturbations due to the presence of noise. While perturbations in the amplitude will be suppressed due to gain saturation, phase perturbations will not be suppressed and therefore will not decay on time. As a result, the oscillator frequency will drift on time. Therefore, in coming to analyze the stability of a given solution to phase perturbations, one should keep in mind that the phase should be marginally stable.

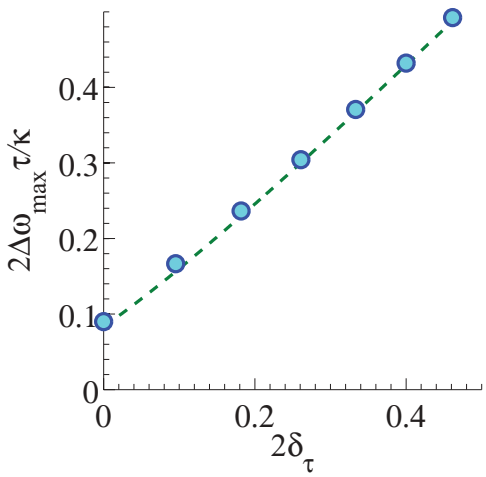

FIG. 5. (Color online) Synchronization region, $2\Delta\omega_{\max}\tau$, as a function of the normalized loop-delay difference, δ_τ, for a $\pi/2$-coupling phase, $\psi = \pi/2$. The analytical results calculated by using Eq. (25) (green-dashed line) are compared with the results of a comprehensive numerical simulation (cyan circles). The rest of the parameters are the same as in Fig. 3.

In this case, phase perturbations do not grow exponentially rather than necessarily decay. The frequency drift of the oscillator may be prevented by locking the oscillator to a reference source.

Let $\delta u_j \ll u_j$ and $\delta\phi_j \ll 1$ be small amplitude and phase perturbations, respectively, to the oscillating phasors that solve for Eqs. (9). The small-signal stability analysis is performed by substituting the perturbed phasors in Eqs. (9) and linearizing the system response to the small perturbations, thus keeping only terms that are linear with $\delta u_j/u_j$ and $\delta\phi_j$, and neglecting higher-order terms. The dynamic equations for the amplitudes and phase perturbations are

$$\begin{aligned}\delta\dot{u}_n &= [\rho_n V_n'(u_n) - 1]\delta u_n/\tau_n + [\rho_n V_n(u_n)k_{jn}/\tau_n] \\ &\quad \times [L_j'(u_j)\cos(\tilde{\gamma}_{jn})\delta u_j - \sin(\tilde{\gamma}_{jn})(\delta\phi_n - \delta\phi_j)], \\ \delta\dot{\phi}_n &= (k_{jn})/\tau_n)\{\sin(\tilde{\gamma}_{jn})[L_n'(u_n)\delta u_n - L_j'(u_j)\delta u_j] \\ &\quad - \cos(\tilde{\gamma}_{jn})(\delta\phi_n - \delta\phi_j)\},\end{aligned} \tag{34}$$

where $n = 1,2$ is the oscillator number, $j = 3 - n$, $L_n(u_n) = \ln[V_n(u_n)]$, and $L_n'(u_n) = V_n'(u_n)/V_n(u_n)$. We define the phasor perturbation vector by

$$(\delta q_1,\delta q_2,\delta q_3,\delta q_4) = (\delta u_1,\delta u_2,\delta\phi_1,\delta\phi_2). \tag{35}$$

The dynamics of the phasor perturbation is described by

$$\delta\dot{q}_i = \sum_{j=1}^{j=4} d_{ij}\delta q_j, \tag{36}$$

where d_{ij} are the elements of matrix **D** that are defined by Eqs. (34)–(36).

According to Eq. (36), the solution is stable or marginally stable to amplitude and phase perturbations if $\lambda_j \leqslant 0$, $j = 1,\ldots,4$, where λ_j are the eigenvalues of the matrix **D**. We note that for the case of two uncoupled oscillators, $s_{12} = s_{21} = 0$, two of the eigenvalues of **D** are both equal to zero, $\lambda_3 = \lambda_4 = 0$. This indicates that the phase noise is accumulated on time without growing or decaying exponentially.

In the case of two identical delay-line oscillators, $\delta_\tau = 0$ and $\Delta\omega = 0$, that are coupled with the $\pi/2$-coupling phase to each other, $\psi = \pi/2$, the solution for the common frequency, Ω, is described by Eq. (31). In the case in which $\Delta\omega = 0$, one solution of the equation which gives $\Omega = 0$ is unstable. In this case, $\Delta\phi = \pm\pi/2$, two eigenvalues of the matrix **D** are negative, $\lambda_{1,2} < 0$, one eigenvalue is zero, $\lambda_3 = 0$, and the last eigenvalue equals

$$\lambda_4 = -[k_{21}\cos(\tilde{\gamma}_{21})/\tau_1 + k_{12}\cos(\tilde{\gamma}_{12})/\tau_2]. \tag{37}$$

If $\Delta\phi = \pi/2$, then $\tilde{\gamma}_{21} = -\pi$ and $\tilde{\gamma}_{12} = 0$. As a result, $\delta_u < 0$, $k_{12} < k_{21}$, and therefore $\lambda_4 = (k_{21} - k_{12})/\tau > 0$. If $\Delta\phi = -\pi/2$, then $\tilde{\gamma}_{21} = 0$, $\tilde{\gamma}_{12} = \pi$, $k_{12} > k_{21}$, and therefore $\lambda_4 = (k_{12} - k_{21})/\tau > 0$. Hence, in the case in which $\Delta\omega = 0$, the solution of Eq. (31) which gives $\Omega = 0$ is unstable. Following the same calculations, the solution branches of Eq. (31) in which $\Omega = \pm\kappa/\tau$ are stable when $\Delta\omega = 0$. For these solutions, $\Delta\phi = 0$, $\lambda_{1,2} < 0$, $\lambda_3 = 0$, and $\lambda_4 = -(k_{21} + k_{12})/\tau < 0$. The common frequencies for these solution branches are located outside the region between the natural frequencies $[\omega_1,\omega_2]$.

B. Instability due to excess gain in low-intensity cavity modes

The presence of a loop delay within an oscillator cavity may enable oscillation in several cavity modes. Limiting the number of cavity modes that can oscillate is usually done by adding an intracavity filter. The central frequency of the filter along with the ratio between its bandwidth and the cavity mode spacing determine which cavity modes can potentially oscillate. In order that a solution will be stable in delay-line oscillators, small perturbations to the amplitudes of low-intensity cavity modes should be suppressed. The frequencies of the low-intensity cavity modes are $\omega_{m,j} = \omega_0 + 2\pi m/\tau_j$ ($m \neq 0$). The close-loop gain $G(u_j)$ of each oscillator is determined by the amplitude of the oscillating mode, u_j. The close-loop gains of the low-intensity cavity modes depend linearly on the close-loop gain of the oscillating mode. Hence, the oscillating mode affects the stability of the low-intensity modes. In this paper, we analyze this effect. We do not perform here a complete stability analysis of the low-intensity modes, and in particular we do not take into account the coupling between those modes. Such a neglect can be justified based on physical considerations since in most practical cases the loop delays of the two oscillators are different. Therefore, the frequencies of the coupled low-intensity cavity modes will not be the same in the two oscillators. Hence, in almost all the practical cases, a low-intensity mode that is injected from one oscillator to another will not fulfill the oscillation condition of the second oscillator. The general stability analysis of the low-intensity modes in cases in which their frequencies overlap is beyond the scope of this paper.

We show that amplitude instability of low-intensity modes can be suppressed by narrowing the filter bandwidth, and we calculate the minimum filter bandwidth that is required. The dynamic equations for the low-intensity modes in an oscillator with a loop delay τ are given by (see Appendix C)

$$\begin{aligned}\dot{a}_m &= a_m(|F(\omega_m)|\Delta^+ - 1)/\tau \\ &\quad + a_{-m}|F(\omega_m)|\Delta^- \cos(\phi_m + \phi_{-m})/\tau, \\ \dot{\phi}_m &= -\frac{a_{-m}}{a_m}\frac{\delta_R}{\tau}\sin(\phi_m + \phi_{-m}) + \frac{\varphi^F(\omega_m)}{\tau},\end{aligned} \tag{38}$$

where $m \neq 0$ is the mode number, $\delta_R = \Delta^-/\Delta^+$, and

$$\Delta^\pm = [V'(a_0) \pm V(a_0)/a_0]/2. \tag{39}$$

To derive an analytic solution to Eqs. (38) and their analytic conditions for stability, we assume that the filter frequency response satisfies $F(\omega_m) \approx F^*(\omega_{-m})$, such that $|F(\omega_m)| \approx |F(\omega_{-m})|$ and $\varphi^F(\omega_m) = -\varphi^F(\omega_{-m})$. Using this assumption and the transformation $\phi_m \to \phi_m + \varphi^F(\omega_m)T/\tau$, we find that in the transformed variables the solutions satisfy $\phi_m + \phi_{-m} = \pi N$ ($m \neq 0$). Let $\delta a_m \ll a_m$ and $\delta\phi_m \ll 1$ be small amplitude and phase perturbations, respectively, to the phasor of the mth cavity mode that solves Eqs. (9). The dynamic equations to the amplitude and phase perturbations of the mth mode, derived in the same manner as was used to obtain Eq. (34), are

$$\delta\dot{a}_m = [(\Delta_m^+ - 1)\delta a_m \pm \Delta_m^-\delta a_{-m}]/\tau, \tag{40}$$

$$\delta\dot{\phi}_m = \mp\frac{1}{\tau}\frac{\Delta^-}{\Delta^+}\frac{a_{-m}}{a_m}(\delta\phi_m + \delta\phi_{-m}), \tag{41}$$

such that

$$\begin{pmatrix}\delta\dot{a}_m\\ \delta\dot{a}_{-m}\end{pmatrix} = \frac{1}{\tau}\begin{pmatrix}\Delta_m^+ - 1 & \pm\Delta_m^-\\ \pm\Delta_m^- & \Delta_m^+ - 1\end{pmatrix}\begin{pmatrix}\delta a_m\\ \delta a_{-m}\end{pmatrix} \tag{42}$$

and

$$\begin{pmatrix}\delta\dot{\phi}_m\\ \delta\dot{\phi}_{-m}\end{pmatrix} = \mp\frac{1}{\tau}\frac{\Delta^-}{\Delta^+}\begin{pmatrix}\chi_{-m} & \chi_{-m}\\ \chi_m & \chi_m\end{pmatrix}\begin{pmatrix}\delta\phi_m\\ \delta\phi_{-m}\end{pmatrix}, \tag{43}$$

where the upper and lower signs corresponds to the solutions $\phi_m + \phi_{-m} = 2\pi N$ and $\phi_m + \phi_{-m} = \pi + 2\pi N$, respectively, $\chi_m = a_m/a_{-m}$, $\Delta_m^\pm = |F(\omega_m)|\Delta^\pm$, and $\Delta^\pm$ are given in Eqs. (39). The eigenvalues of the matrices in Eqs. (42) and (43) are

$$\begin{aligned}\lambda_{a_m,1} &= \Delta_m^+ + \Delta_m^- - 1,\\ \lambda_{a_m,2} &= \Delta_m^+ - \Delta_m^- - 1\end{aligned} \tag{44}$$

and

$$\begin{aligned}\lambda_{\phi_m,1} &= 0,\\ \lambda_{\phi_m,2} &= \mp\frac{\Delta^-}{\Delta^+}\left(\frac{a_m}{a_{-m}} + \frac{a_{-m}}{a_m}\right),\end{aligned} \tag{45}$$

respectively. The solution is locally or marginally stable to amplitude and phase perturbations if $\lambda_{a_m,j} \leqslant 0$ and $\lambda_{\phi_m,j} \leqslant 0$. We note that $\lambda_{\phi_m,2} \leqslant 0$ if $V' \geqslant V(a_0)/a_0$ and $\phi_m + \phi_{-m} = 2\pi N$ or if $V(a_0)/a_0 \geqslant V'$ and $\phi_m + \phi_{-m} = \pi + 2\pi N$. The stability is therefore determined by $\lambda_{a_m,j}$, such that the solution is stable to perturbations in low-intensity cavity modes if

$$|F(\omega_m)|V'(a_0) = |F(\omega_m)|[G'(a_0)a_0 + G(a_0)] \leqslant 1 \tag{46}$$

and

$$|F(\omega_m)|V(a_0)/a_0 = |F(\omega_m)|G(a_0) \leqslant 1. \tag{47}$$

Thus, instability can be suppressed by narrowing the bandwidth of the filter.

We consider the case of two similar delay-line oscillators that are coupled with the $\pi/2$-coupling phase to each other, as described in Sec. III B. We would like to show that if the filter is wide enough, such that $|F(\omega_{m,j})| \approx 1$, where $\omega_{m,j}$ is the frequency of a low-intensity cavity mode, $m \neq 0$, then the synchronized solution becomes unstable even if $\omega_1 = \omega_2$. In this case, $\Delta\omega = 0$, and according to Eq. (23), if $\tau_1 \neq \tau_2$, then $\Delta u_1 \Delta u_2 < 0$, and we can assume without the loss of generality that

$$u_1 < u^0 < u_2. \tag{48}$$

The free-running oscillating amplitude is stable, and therefore $G(u^0) = 1$, $G'(u^0) < 0$, and

$$G(u_2) < 1 < G(u_1). \tag{49}$$

Therefore, since $|F(\omega_{m,j})| \approx 1$, we get that $[G(u_1)]|F(\omega_{m,1})| > 1$. As a result, the amplitude of this cavity mode in loop 1 will increase in each round trip and the solution will become unstable in accordance with Eq. (47). It can be concluded that it is possible to obtain synchronization between two OEOs that are coupled with the $\pi/2$-coupling phase, provided that the filter is sufficiently narrow and the detuning between the natural frequencies of the delay-line oscillators is sufficiently small.

VII. CONCLUSION

We have derived a model for studying two weakly coupled delay-line oscillators. By assuming a weak coupling and performing a linear approximation to the interaction between the two oscillators, we derived coupled equations that accurately describe the two weakly coupled delay-line oscillators. We derived analytical solutions for the equations in the case of two similar delay-line oscillators with the zero- and the $\pi/2$-coupling phase. We show that in the case of the $\pi/2$-coupling phase, there are two terms that contribute to the synchronization region, a term that is linearly dependent on the coupling parameter, and another term that is quadratically dependent on the coupling parameter. The physical effect of the quadratic term enables the synchronization of the two delay-line oscillators in cases in which only the linear term would not allow. The quadratic term cannot be derived by phase-oscillator models that omit the amplitude dynamics. Therefore, the amplitude response should be retained even if the two delay-line oscillators are weakly coupled to each other. We show that the presence of low-intensity cavity modes should be taken into account in the stability analysis of two weakly coupled delay-line oscillators.

We used the delay-line oscillator model to study the conditions under which a synchronized continuous-wave signal can be obtained by two weakly coupled OEOs. We analyze the effect of the coupling phase on the synchronization properties of OEOs. In particular, we explain why two identical OEOs that are weakly coupled to each other with a $\pi/2$-coupling phase can be synchronized, even though this result is in contrast to that of phase-oscillator models. The results of the model are compared with the results of a comprehensive numerical simulation for two coupled OEOs. A very good quantitative agreement is achieved between the results for two weakly coupled delay-line oscillators. We intend to verify experimentally the results that are presented in this paper in two coupled OEOs.

ACKNOWLEDGMENTS

This work was supported by the Israel Science Foundation (ISF) of the Israeli Academy of Sciences (Grant No. 1092/10).

APPENDIX A: DYNAMIC EQUATIONS FOR THE OSCILLATING SIGNAL ($M = 0$) IN A SINGLE-MODE APPROXIMATION

We start with the expansion of $x_j^c(T)$ into a series of modes with amplitudes a_m as described in Eq. (3). We assume that most of the signal energy is contained in a single oscillating mode, a_0, such that $a_{0,j}^2 \gg \sum_{m\neq 0} a_{m,j}^2$, and we can treat the low-intensity modes, $m \neq 0$, as small perturbations to the amplitude and phase of the oscillating phasor. By using the approximation

$$\begin{aligned}A\exp(i\alpha) + B\exp(i\beta) \approx A[1 + (B/A)\cos(\beta - \alpha)]\exp\{i[\alpha\\ + (B/A)\sin(\beta - \alpha)]\},\end{aligned} \tag{A1}$$

where A, B, α, β are real numbers and $B \ll A$, we obtain from Eq. (3)

$$|x_j^c(T)| \approx a_{0,j} + \sum_{m\neq 0} a_{m,j}\cos[\zeta_{m,j}(T)],$$
$$\phi_j(T) \approx \phi_{0,j} + \sum_{m\neq 0} (a_{m,j}/a_{0,j})\sin[\zeta_{m,j}(T)], \tag{A2}$$

where $\zeta_{m,j}(T) = \Omega_{m,j}t + \phi_{m,j}$. The phasor at the output of the saturable amplifier is given by

$$x_j^G(T) = G\big[\big|x_j^c(T)\big|\big]x_j^c(T). \tag{A3}$$

The single-mode approximation that is used in Eqs. (A2) is relevant for many practical applications of delay-line oscillators, and it is important even in cases in which there is cavity-mode competition at start-up [30]. In this case, one of the cavity modes starts oscillating and the small signal gain of the other cavity modes decreases due to gain saturation. The noise that is present when the oscillator is turned on determines the specific mode that will oscillate at steady state, and the mode with the highest gain has the highest probability to be selected [30]. For most practical cases, it is usually justified to assume that the oscillation frequency ω_0 is located near the peak of $F_j(\omega)$, such that $F_j(\omega_0) \approx 1$ for both $j = 1,2$. Therefore, we assume that $[\varphi_j^F(\omega_j) - \varphi_j^F(\omega_0)]/\tau_j \ll \omega_j - \omega_0$. The phase response of the filter can be kept in the dynamic equations by replacing θ_j by $\theta_j + \varphi_j^F(\omega_0)$.

We derive the equations for the oscillating mode by keeping only the oscillating mode term in Eq. (A2), for $m = 0$, and omitting the presence of the other cavity modes. The amplitude and phase of the oscillating phasors are given by u_j and ϕ_j, respectively, such that

$$x_j^c(T) = u_j(T)\exp[i\phi_j(T)], \tag{A4}$$

and $u_j \cong a_{0,j}$, $\phi_j \cong \phi_{0,j}$, and j is the oscillator number. The oscillating signals are given by

$$s_j^c(t,T) = u_j(T)\exp[i\varphi_j(t,T)]/2 + \text{c.c.}, \tag{A5}$$

where $\varphi_j(t,T) = \omega_0 t + \phi_j(T)$.

The change in the oscillating phasor from one round trip to the following are calculated by using Eqs. (2), (A3), (A4), and by assuming $F_j(\omega_0) = 1$. Thus, we get the two complex equations:

$$u_n(T)\exp[i\varphi_n(t)] = \rho_n V_n[u_n(T_n)]\exp[i\varphi_n(t_n) + \theta_n] + \kappa_j V_j[u_j(T_j)]\exp[i\varphi_j(t_j) + \psi_j], \tag{A6}$$

where $n = 1,2$, is the oscillator number, $j = 3 - n$, and $T_n = T - \tau_n$, $t_n = t - \tau_n$ are the retarded long time scale, T, and short time scale, t. We define the coupling coefficients by $k_{jn}(T) = \kappa_j V_j[u_j(T)]/\{\rho_n V_n[u_n(T)]\}$. Using the weak-coupling approximation, $k_{jn} \ll 1$, and the approximation in Eq. (A1), we obtain

$$u_n(T)\exp[i\varphi_n(t)] \approx \rho_n V_n[u_n(T_n)]\{1 + k_{jn}\cos[\gamma_{jn}(t)]\} \times \exp\left(i\{\varphi_n(t_n) + \theta_n - k_{jn}\sin[\gamma_{jn}(t)]\}\right), \tag{A7}$$

where

$$\gamma_{jn}(t) = \varphi_n(t - \tau_n) - \varphi_j(t - \tau_j) + \theta_n - \psi_j. \tag{A8}$$

The changes per round trip are approximated by the time derivatives, such that $\dot{u}_j \approx [u_j(T) - u_j(T_j)]/\tau_j$ and $\dot{\phi}_j \approx [\phi_j(T) - \phi_j(T_j)]/\tau_j$. Thus, we obtain

$$\dot{u}_n = u_n[\rho_n V_n(u_n)/u_n - 1]/\tau_n + [\kappa_j V_j(u_j)/\tau_n]\cos[\gamma_{jn}(T)],$$
$$\dot{\phi}_n = 2\pi N_n/\tau_n - \omega_0 - (k_{jn}/\tau_n)\sin[\gamma_{jn}(T)] + \theta_n/\tau_n, \tag{A9}$$

when N_n are integers, and

$$\gamma_{jn}(T) = \omega_0(\tau_j - \tau_n) + \theta_n - \psi_j + \phi_n(T) - \phi_j(T). \tag{A10}$$

Using the requirement that ω_j are the natural frequencies of the two oscillators, we obtain that $2\pi N_n/\tau_n = \omega_n$ and the dynamic equations become

$$\dot{u}_n = u_n[\rho_n V_n(u_n)/u_n - 1]/\tau_n + [\kappa_j V_j(u_j)/\tau_n]\cos[\gamma_{jn}(T)],$$
$$\dot{\phi}_n = \omega_n - \omega_0 - (k_{jn}/\tau_n)\sin[\gamma_{jn}(T)] + \theta_n/\tau_n, \tag{A11}$$

APPENDIX B: COMPREHENSIVE NUMERICAL SIMULATION PARAMETERS FOR SIMULATING COUPLED OEOS

The small-signal open-loop gain of an OEO, G_S, is given by [22,30]

$$G_S = -\frac{\eta\pi v_{\text{ph}}}{v_\pi}\cos(\pi v_B/v_\pi), \tag{B1}$$

where the photodetector voltage is calculated as

$$v_{\text{ph}} = \frac{\alpha P_0 \rho R G_A}{2}, \tag{B2}$$

and P_0 is the input optical power, α is the insertion loss of the MZM, v_π is the modulator half-wave voltage, v_B is the dc bias voltage, η is a parameter determined by the extinction ratio of the modulator, $(1+\eta)/(1-\eta)$, ρ is the responsivity of the photodetector, R is the impedance at the output of the detector, and G_A is the amplifier voltage gain. We note that the voltage v_{ph} is the voltage at the output of the amplifier when the modulator is biased with $v_B = v_\pi$ and its rf port is not connected [30].

Each OEO was modeled as described in detail in [30]. The rf filter has a Lorentzian line shape with a full width at half-maximum bandwidth of Γ. The simulation parameters, unless otherwise specified, were chosen as follows: $P_0 = 10$ mW, $\alpha = 1$, $v_\pi = \pi$, $v_B = v_\pi$, $\eta = 1$, $\rho = 0.8$ A/W, $R = 50\Omega$, $G_A = 5.5$, $\tau = 1$ μs, and $\Gamma = 2/\tau$. The rf filter bandwidth, Γ, was chosen to be narrow enough to avoid the presence of instabilities due to excess gain in other cavity modes, as is discussed in Sec. VI B. A white noise with a spectral density of -160 dB m/Hz was added to the signal at the input of the amplifier in each round trip. The small-signal open-loop gain was $G_S = 1.1$ and the average oscillation power at the output of the amplifier was $P_{\text{osc}} = 7.5$ mW in the free-running case. The coupling coefficients were $\kappa_j = 0.01$, $\theta_j = 0$, and

$\psi_j = 0$ or $\psi_j = \pi/2$, and $\rho_j = 1 - \kappa_j$ or $\rho_j = (1 - \kappa_j^2)^{1/2}$, respectively.

APPENDIX C: DYNAMIC EQUATIONS FOR THE LOW-INTENSITY CAVITY MODES ($m \neq 0$)

In this Appendix, we derive the dynamic equations for the low-intensity cavity modes, $m \neq 0$, in the presence of the oscillating mode, $m = 0$. The dynamic equations are derived for each loop separately, neglecting the coupling effect. We write the oscillating signal according to Eqs. (A2) in the presence of a small perturbation due to the mth cavity mode:

$$\begin{aligned} |x_j^c(T)| &\approx a_{0,j} + a_{m,j}\cos[\zeta_{m,j}(T)], \\ \phi_j(T) &\approx \phi_{0,j} + (a_{m,j}/a_{0,j})\sin[\zeta_{m,j}(T)]. \end{aligned} \tag{C1}$$

The complex envelop, or the phasor, of the oscillating signal with the angular frequency ω_0 is given by $x_j^c(T) = |x_j^c(T)|\exp[i\phi_j(T)]$.

The phasor at the amplifier output, $x^G(T)$, can be calculated by linearizing the amplifier response around the amplitude of the oscillating mode, a_0, and treating the other low-intensity modes, $m \neq 0$, as small perturbations to the oscillation. Thus, using Eqs. (A3) and (C1),

$$\begin{aligned} x^G(T) = &\{V(a_0) + a_m V'\cos[\zeta_m(T)]\} \\ &\times \exp\{i a_m/a_0 \sin[\zeta_m(T)]\}, \end{aligned} \tag{C2}$$

where we omitted the subscript j for the sake of brevity. Using the Jacobi-Anger expansion [36], and keeping terms on the order of a_m/a_0, we obtain

$$\begin{aligned} x^G(T) = &\{V(a_0) + a_m V'\cos[\zeta_m(T)]\} \\ &\times\{J_0(a_m/a_0) + 2i J_1(a_m/a_0)\sin[\zeta_m(T)]\}, \end{aligned} \tag{C3}$$

where $J_0(x)$ and $J_1(x)$ are the zero- and first-order Bessel functions, respectively. Approximating $J_0(x) \approx 1$ and $J_1(x) \approx x/2$ when $x \ll 1$, we get that

$$\begin{aligned} x^G(T) = &V(a_0) + a_m\Delta^+\exp[i\zeta_m(T)] \\ &+ a_m\Delta^-\exp[-i\zeta_m(T)], \end{aligned} \tag{C4}$$

where

$$\Delta^\pm = [V'(a_0) \pm V(a_0)/a_0]/2. \tag{C5}$$

Thus, the change in the phasor of the mth cavity mode in a round trip equals

$$v_m(T+\tau) = F(\omega_m)[\Delta^+ v_m(T) + \Delta^- v_{-m}^*(T)], \tag{C6}$$

where $v_m(T) = a_m(T)\exp[i\zeta_m(T)]$. Assuming that $\delta_R \equiv \Delta^-/\Delta^+ \ll 1$ such that the change of the phasor per round trip is small, then

$$\begin{aligned} v_m(T+\tau) = a_m|F(\omega_m)|\Delta^+ &\left[1 + \frac{a_{-m}}{a_m}\delta_R\cos(\phi_m + \phi_{-m})\right] \\ &\times \exp\left\{i\left[\Omega_m T + \phi_m - \frac{a_{-m}}{a_m}\delta_R\sin(\phi_m + \phi_{-m})\right.\right. \\ &\left.\left. + \varphi^F(\omega_m)\right]\right\}, \end{aligned} \tag{C7}$$

where $F(\omega_m) = |F(\omega_m)|\exp[i\varphi^F(\omega_m)]$. As a result, the dynamic equations of the mth cavity mode are

$$\begin{aligned} \dot{a}_m = &a_m[|F(\omega_m)|\Delta^+ - 1]/\tau \\ &+ a_{-m}|F(\omega_m)|\Delta^-\cos(\phi_m + \phi_{-m})/\tau, \end{aligned} \tag{C8}$$

$$\dot{\phi}_m = -\frac{a_{-m}}{a_m}\frac{\delta_R}{\tau}\sin(\phi_m + \phi_{-m}) + \frac{\varphi^F(\omega_m)}{\tau}. \tag{C9}$$

[1] R. Adler, Proc. IRE **34**, 351 (1946); Proc. IEEE **61**, 1380 (1973).
[2] K. Kurokawa, IEEE Trans. Microwave Theory Tech. **16**, 234 (1968).
[3] W. O. Schlosser, IEEE Trans. Microwave Theory Tech. **16**, 732 (1968).
[4] R. A. York, IEEE Trans. Microwave Theory Tech. **41**, 1799 (1993).
[5] A. Banai and F. Farzaneh, IEE Proc., Microw. Antennas Propag. **147**, 13 (2000).
[6] D. G. Aronson, G. B. Ermentrout, and N. Kopell, Physica D **41**, 403 (1990).
[7] Y. Kuramoto, in *International Symposium on Mathematical Problems in Theoretical Physics*, Vol. 39, edited by H. Araki (Springer-Verlag, Berlin, 1975); *Chemical Oscillations, Waves, and Turbulence* (Springer-Verlag, Berlin, 1984).
[8] M. K. Stephen Yeung and S. H. Strogatz, Phys. Rev. Lett. **82**, 648 (1999).
[9] H. G. Schuster and P. Wagner, Prog. Theor. Phys. **81**, 939 (1989).
[10] S. Kim, S. H. Park, and C. S. Ryu, Phys. Rev. Lett. **79**, 2911 (1997).
[11] D. H. Zanette, Phys. Rev. E **62**, 3167 (2000).
[12] T. W. Ko and G. B. Ermentrout, Phys. Rev. E **76**, 056206 (2007).
[13] G. C. Sethia, A. Sen, and F. M. Atay, Phys. Rev. E **81**, 056213 (2010).
[14] D. V. Ramana Reddy, A. Sen, and G. L. Johnston, Phys. Rev. Lett. **80**, 5109 (1998).
[15] D. V. Ramana Reddy, A. Sen, and G. L. Johnston, Physica D **129**, 15 (1999).
[16] M. B. Spencer and W. L. Lamb, Phys. Rev. A **5**, 893 (1972).
[17] R. Kuske and T. Erneux, Opt. Commun. **139**, 125 (1997).
[18] T. Heil, I. Fischer, W. Elsässer, J. Mulet, and C. R. Mirasso, Phys. Rev. Lett. **86**, 795 (2001).
[19] J. Javaloyes, P. Mandel, and D. Pieroux, Phys. Rev. E **67**, 036201 (2003).
[20] H. J. Wünsche, S. Bauer, J. Kreissl, O. Ushakov, N. Korneyev, F. Henneberger, E. Wille, H. Erzgräber, M. Peil, W. Elsäßer, and I. Fischer, Phys. Rev. Lett. **94**, 163901 (2005).
[21] H. Erzgräber, D. Lenstra, B. Krauskopf, E. Wille, M. Peil, I. Fischer, and W. Elsäßer, Opt. Commun. **255**, 286 (2005).
[22] X. S. Yao and L. Maleki, J. Opt. Soc. Am. B **13**, 1725 (1996).

[23] X. S. Yao and L. Maleki, IEEE J. Quantum Electron. **36**, 79 (2000).
[24] W. Zhou and G. Blasche, IEEE Trans. Microwave Theory Tech. **53**, 929 (2005).
[25] E. C. Levy, O. Okusaga, M. Horowitz, C. R. Menyuk, W. Zhou, and G. M. Carter, Opt. Express **18**, 21461 (2010).
[26] M. Peil, L. Larger, and I. Fischer, Phys. Rev. E **76**, 045201 (2007).
[27] M. Grapinet, V. S. Udaltsov, L. Larger, and J. M. Dudley, Electron. Lett. **44**, 764 (2008).
[28] R. Lavrov, M. Peil, M. Jacquot, L. Larger, V. S. Udaltsov, and J. M. Dudley, Phys. Rev. E **80**, 026207 (2009).
[29] Y. K. Chembo, L. Larger, and P. Colet, IEEE J. Quantum Electron. **44**, 858 (2008).
[30] E. C. Levy, M. Horowitz, and C. R. Menyuk, J. Opt. Soc. Am. B **26**, 148 (2009).
[31] E. Rubiola, *Phase Noise and Frequency Stability in Oscillators* (Cambridge University Press, New York, 2009), Chap. 3, p. 67.
[32] A. S. Besicovitch, *Almost Periodic Functions* (Dover, New York, 1954).
[33] A. F. Wickersham, Jr., J. Opt. Soc. Am. **48**, 958 (1958).
[34] L. Mandel and E. Wolf, *Optical Coherence and Quantum Optics* (Cambridge University Press, Cambridge, 1995), Chap. 10, Sec. 9.5 p. 511.
[35] H. K. Khalil, *Nonlinear Systems* (Prentice-Hall, Englewood Cliffs, NJ, 2000), Chap. 4, p. 111.
[36] F. W. J. Olver, in *Handbook of Mathematical Functions*, edited by M. Abramowitz and I. A. Stegan (Dover, New York, 1972), Chap. 9, p. 355.